Journal Name

ARTICLE TYPE

CO_2 capture by pumping surface acidity to the deep ocean†

Michael D. Tyka,*[a] Christopher Van Arsdale,[a] and John C. Platt[a]

This paper is a non-peer reviewed preprint submitted to EarthArXiv. It has been submitted to Energy & Environmental Science.

The majority of IPCC scenarios call for active CO_2 removal (CDR) to remain below 2ºC of warming. On geological timescales, ocean uptake regulates atmospheric CO_2 concentration, with two homeostats driving CO_2 uptake: dissolution of deep ocean calcite deposits and terrestrial weathering of silicate rocks, acting on 1ka to 100ka timescales, respectively. Many current ocean-based CDR proposals effectively act to accelerate the latter. Here we present a method which relies purely on the redistribution and dilution of acidity from a thin layer of the surface ocean to a thicker layer of deep ocean, with the aim of reducing surface acidification and accelerating the former carbonate homeostasis. This downward transport could be seen analogous to the action of the natural biological carbon pump. The method offers advantages over other ocean CDR methods and direct air capture approaches (DAC): the conveyance of mass is minimized (acidity is pumped in situ to depth), and expensive mining, grinding and distribution of alkaline material is eliminated. No dilute substance needs to be concentrated, avoiding the Sherwood's Rule costs typically encountered in DAC. Finally, no terrestrial material is added to the ocean, avoiding significant alteration of seawater ion concentrations or issues with heavy metal toxicity encountered in mineral-based alkalinity schemes. The artificial transport of acidity accelerates the natural deep ocean compensation by calcium carbonate. It has been estimated that the total compensation capacity of the ocean is on the order of 1500GtC. We show through simulation that pumping of ocean acidity could remove up to 150GtC from the atmosphere by 2100 without excessive increase of local ocean pH. For an acidity release below 2000m, the relaxation half-life of CO_2 return to the atmosphere was found to be $\sim$2500 years ($\sim$1000yr without accounting for carbonate dissolution), with $\sim$85% retained for at least 300 years. The uptake efficiency and residence time were found to vary with the location of acidity pumping, and optimal areas were determined. Requiring only local resources (ocean water and energy), this method could be uniquely suited to utilize otherwise-unusable open ocean energy sources at scale. We examine technological pathways that could be used to implement it and present a brief techno-economic estimate of 130-250\$/tCO_2 at current prices and as low as 93\$/tCO_2 under modest learning-curve assumptions.

1 Introduction

Stabilizing the earth's climate into the next centuries will require a near total decarbonization of the world energy supply, i.e. reducing emissions from their current peak levels. However, some industrial processes, such as industrial heat and concrete manufacturing as well as emissions from land use changes, air travel, or livestock are very difficult to decarbonize[1]. Further, even if future emissions were curbed, enough historical CO_2 has already accumulated in the atmosphere to cause problematic warming and could trigger tipping points. Thus, the vast majority of IPCC

[a]*Google Inc., 601 N 34th St, Seattle, WA 98103, USA; E-mail: mike.tyka@gmail.com*

† Electronic Supplementary Information (ESI) available: [details of any supplementary information available should be included here].

RCP2.6 scenarios which remain under 2ºC of warming require negative emissions on the order of 150GtC before 2100[2,3] in addition to rapid decarbonization. On geological timescales several mechanisms act to regulate the atmospheric CO_2 concentration: Over periods of hundreds of years the oceans will absorb the majority of the excess CO_2 leading to very significant surface acidification[4]. Subsequent downward transport of the CO_2 brings the acidity in contact with $CaCO_3$ deposits, dissolving them and releasing alkalinity, and thus stabilizing the pH. This has been termed the $CaCO_3$ pH-stat[5]. On even longer timescales (100ka), weathering of terrestrial silicate rocks releases additional alkalinity which brings new alkalinity to the oceans and allows the previously dissolved $CaCO_3$ to be redeposited while the lysoclines return to their original depths. This is termed the CO_2 weathering stat. The consecutive transfer of the excess CO_2 along these three sinks acts to keep the temperature of the earth within relatively stable bounds over long periods of time[6,7]. Unfortunately, the response time of even the first of these two buffers is too slow to keep up with the rate of human emissions[8,9], leading to a temporary but extremely dangerous spike in atmospheric CO_2 concentrations, warming and surface ocean acidification, potentially triggering mass extinction.

The primary limiting step is the net transport of CO_2 into the deep ocean due to the action of the biological pumps[10]. Anthropogenic CO_2 has not yet penetrated deeply into the ocean, because most of the remineralization of sinking organic matter occurs in the first 500m beyond the euphotic zone, with peak acidification at about 250m depth[4]. Anthropogenic CO_2 has acidified mostly surface waters, impacting carbonate shell-forming organisms, while staying out of reach of inorganic $CaCO_3$ deposits located well below the euphotic zone[11]. Positive feedbacks are also present in this system, where CO_2-saturated surface wates oppose further CO_2 uptake, reduce the ocean buffering ability and accelerate future pH changes due to the nonlinearity of the carbonate system[12]; these issues are further compounded under increasing stratification and a decreased biological pump predicted for a warming ocean.

While methods have been proposed to accelerate the terrestrial CO_2-weathering stat[2,13], by mechanical[14,15] or electrochemical means[16,17], acceleration of the $CaCO_3$ pH-stat has not yet been explored. Here, we examine the feasibility of artificially accelerating the transport of acidity to the deep ocean, in order to dilute the surface acidification and enable the action of the natural carbonate compensation on accelerated timescales. Such an action cannot be a replacement for total decarbonization of the economy, but could contribute to blunt the ecological impact of past emissions by dilution in spatial and temporal dimensions. The inventory of erodible $CaCO_3$ on the ocean floor is estimated to be ~1600 GtC[8], theoretically more than sufficient to compensate for the ~640GtC that humanity has released since pre- industrial times.

1.1 Accelerating deep water equilibration

We envision an artificial method to increase the downward transport of acidity from the surface ocean to the deep ocean that first involves electrochemically splitting seawater into acid and base. The weakly alkaline effluent would be released at the surface, while the weakly acidic water would be pumped into the deep ocean (see Figure 1). In the surface water the alkalinity would thus be raised and the pH stabilized. This maintains an increased flux of CO_2 into the ocean and reduces atmospheric CO_2, helping to alleviate immediate radiative forcing. The increased pH (decreased acidity) would also help stabilize the health of coral reefs and Coccolithophores and help preserve these ecosystems past the anthropogenic CO_2 spike. Synthesis and subsequent sinking of coccoliths plays a vital role in ballast formation in the biological pump and indirectly aids the downward transport of organic carbon in the ocean[18]. These surface-ocean effects would be the same as those of ocean liming proposals[13], i.e. surface dissolved inorganic carbon (DIC) would increase together with an equally increased alkalinity and the carbonate equilibrium would remain stable. A common approximation[10] for the concentration of carbonate ions is $[CO_3^{2-}] \approx Alk - DIC$, which makes this immediately apparent. Meanwhile the acidic, low-pH effluent could be diluted across a large section of the deep water column using perforated, flexible, deep vertical pipes. As the deep water column contains much more water than the thin surface water layer that the acidity originated in, such redistribution of surface-ocean acidity dilutes the surface acidity and its ecological effects. Isopycnal deep water circulation would then spread and dilute this acidity horizontally, bringing it in contact with calcite sediments. The precise impact of such a redistribution on pH and calcite saturation is complex and will be explored through ocean simulation in this paper.

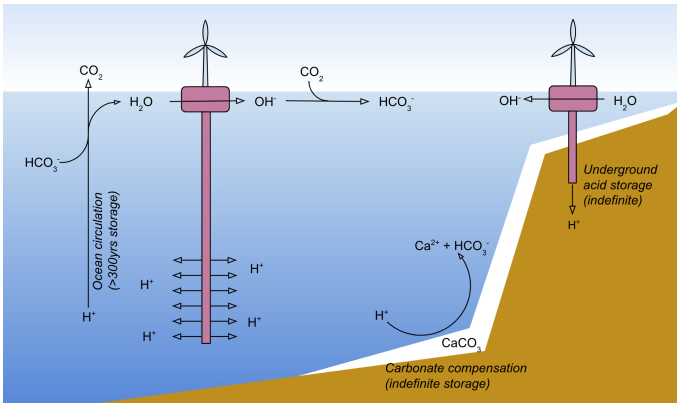

Fig. 1 Schematic showing how pumping of acidity from surface water would accelerate the natural pH stat of the ocean, help stabilize atmospheric CO_2 and accelerate deep water carbonate compensation. Any unreacted acidity would eventually return with ocean circulation. Alternatively, for shallow ocean areas, acidity could be pumped into underground basalt formations or depleted oil reservoirs, leading to permanent CO_2 drawdown into the ocean.

1.1.0.1 Comparison with mineral alkalinization

A great variety of methods have been proposed to increase ocean capacity for CO_2, without raising ocean acidity, by dissolving terrestrial minerals[13]. These proposals aim to accelerate the terrestrial weathering CO_2-stat by about 5-6 orders of magnitude. In practice, the mining, grinding, transport and distribution of gigatonnes of rock per year poses significant challenges. If the mate-

rial is ground to $\sim$100μm, the dissolution of these minerals is on the order of many decades[14,15] and particles would sink out of the mixed layer long before dissolution[21], limiting applicability to shallow coastal areas[22]. Grinding down to 1μm would enable open ocean distribution, but significantly increase grinding energy costs[23]. Iron, abundant in most olivine minerals, would inadvertently fertilize the ocean leading to significant ecological disruption[2,14]. Silicates would shift the phytoplankton species composition towards diatoms[21] and heavy metals (Nickel, Cadmium, etc) would exhibit acute toxicity and potentially bioaccumulate. Thus these co-dissolving contaminants likely limit deployment at the scale needed ($\sim$150GtC before 2100). To solve these problems a number of methods have been put forward which extract alkalinity from rocks without adding bulk rock to the oceans. Typically, ocean-derived brine is split into acid and base electrochemically[16,17,24]. The base can be added to the surface ocean, while the excess acid can be neutralized using rocks on land. This also circumvents the need for expensive fine grinding, but the negative impacts of mining itself remain.

This proposal shares many properties with the above ocean alkalinity enhancement proposals, with some advantages. Firstly there is no need for large mass transport of alkaline rocks to the ocean[13] or transport of products away from electrolysers[24]. The only matter transport needed is the pumping of a small amount of water a few kilometers downwards. This locality makes the method uniquely suitable for open ocean deployment and provides a way to use otherwise unusable renewable energy resources. Open waters offer greater scalability at reduced ecological impact as dilution over large areas is trivial and marine ecosystems are much sparser. The proposed method also avoids the severe impacts of creating a gigatonne-scale mining operation on terrestrial ecosystems. The net cation composition of the ocean is not changed, avoiding introduction of iron, silicate or toxic trace metals into ocean ecosystems, a major concern with most mineral-based alkalinization approaches[2]. The redistribution of alkalinity dilutes the already occurring anthropogenic acidification of the surface ocean into the deeper ocean. Due to these advantageous ecological properties, the proposed method may find it easier to gain support and acceptance from the public, as it aims to mitigate human impact by spatial and temporal dilution.

We note also that widely discussed biological ocean CDRs[25] which propose increasing primary biological productivity and sinking of biological matter, such as ocean fertilization, could be seen as equivalent to the acidity pumping proposed here. This is because the vast majority of sunk soft tissue is remineralized in the water column or on the ocean floor, thus acidifying deep waters[26]. Only 0.4% of the originally fixed carbon is buried in sediments and permanently removed from circulation[10]. Thus efforts increasing primary biological production likewise rely on the dissolution of deep $CaCO_3$ deposits to prevent the transported carbon from being re-emitted to the atmosphere on the timescales of ocean circulation. Thus, these methods also aim to accelerate the carbonate pH-stat, albeit indirectly. The same can be said for efforts to directly inject CO_2 into the deep sea, as the resulting CO_2 lakes or hydrates gradually dissolve[27].

In this paper we present ocean circulation simulations to examine the effects and limitations of large-scale acidity pumping as well as techno-economic arguments which suggest that the cost per tonne of CO_2 could potentially be competitive with terrestrial direct air capture (DAC) and other negative emissions technologies while avoiding the ecological impacts of accelerated mineral weathering[2].

2 Methods

2.1 Global Circulation Model of acid-base pumping

To simulate the effect of acid-base pumping on surface and deep water pH, as well as net ocean CO_2 uptake, and evaluate the return time of acidity, we used a full ocean circulation model in a 128x64 worldwide spherical polar grid using MITgcm[28]. The simulation had cell sizes of 2.8°$\times$2.8° divided into 20 exponentially spaced depth levels, from 10m thick at the surface to 690m thick at depth. The simulation was initialized and forced as detailed in Dutkiewicz et al. 2005[29]. The MITgcm GEOM and DIC modules were used to simulate the soft tissue and carbonate pumps, as well as ocean-atmosphere gas exchange. A number of studies[30,31] have simulated addition of alkalinity to the ocean in the context of realistic emission scenarios with increasing atmospheric pCO_2. Here we chose to focus instead on the efficiency of CO_2 uptake and the circulation aspects of acidity return, and thus the atmospheric concentration of CO_2 was simply held constant at 415ppm similar to work by Kähler et al.[21].

2.1.1 Perturbation.

Custom code was added to simulate the transport of alkalinity from a parameterizable slab of deep water to the top 10m of surface water corresponding to the pumping of acidity in the opposite direction, keeping the total ocean alkalinity constant. To investigate the fate of alkalinity and acidity separately, some simulations were modified to only alkalize, in which case the total alkalinity change was not conservative. These simulations srepresent an idealized addition of pure alkalinity to the surface ocean. In all experiments the pumped alkalinity was released into the top 10m slab, but the acid-injection slab position and thickness, as well as the distribution of pumping, were varied from experiment to experiment, as detailed in the results section. The movement of volume was not explicitly modelled, as the involved quantities are tiny ($\sim 5\times10^{-3}$ Sv/GtC) compared to the natural ocean overturning.

2.1.2 Carbonate compensation.

The return of the acidity with the overturning circulation is the timeframe in which the transported acidity can be neutralized by dissolving carbonate sediments. Both the dissolution of existing $CaCO_3$ deposit inventories (estimated[6] at a total of 1600GtC), and reduction of new carbonate deposition (estimated at 0.27GtC/yr to 0.1GtC/yr[32,33]) increase net alkalinity in the ocean and would act to neutralize any pumped acidity. Due to the relatively short amount of time that sinking particles spend in the water column, most of the dissolution below the carbonate saturation horizon (CSD) occurs on the ocean floors. Despite the relatively uncertain current carbonate dissolution rates (0.3GtC/yr

$\pm$60%)[11] a basic model of increased carbonate compensation due to pumped acidity can be constructed. The rate r of seafloor dissolution has been expressed[34,35] as

$$r = k^*([CO_3{}^{2-}]_{sat} - [CO_3{}^{2-}]) \quad (1)$$

The effective rate constant, k^*, is limited by sediment-side mass transport (K_s) or water-side diffusion (β) through a boundary layer, whichever is slower[34,35]:

$$k^* = K_s\beta/(K_s+\beta) \quad (2)$$

Most locations of significant (>20%) carbonate content are limited by water-side diffusion[11], as bottom water speeds are relatively slow. Thus the resulting kinetics are linear with respect to the carbonate ion concentration and relatively independent of sediment $CaCO_3$ content. To simulate the dissolution of $CaCO_3$ deposits during our simulations, a gridded map of dissolution rate constant, k* and sedimentary $CaCO_3$ content was obtained from work by Sulpius et al.[11]. The bottom dissolution rate was then calculated by equation 1 for all grid tiles where the $CaCO_3$ fraction > 10%. For grid tiles containing less than 10% the dissolution rate was set to 0. At the same time, any biological carbonate flux reaching the ocean floor was modelled to have settled onto the seafloor. At steady state the rate of sedimentation and dissolution was found to be relatively balanced, i.e. the total ocean alkalinity was not changing rapidly. Riverine alkalinity input was not modelled. An initial simulation allowed the ocean system to equilibrate for 2500 years and was used as the starting point for all subsequent pumping simulations. All the simulation setups, code modifications and parameters are available?

3 Results

3.1 Uniform pumping

In our initial simulations alkalinity was pumped uniformly over the entire ocean, wherever the respective depth was available to pump acidity to. The amount of alkalinity pumped was 0.25Pmol/yr the equivalent to a maximum uptake of 3GtCeq/yr, roughly the same amount as was used by[21]. Note that throughout this paper we will use units of 1GtCeq=0.833Tmol to provide a better intuitive sense for the quantities involved (relative to human emissions of ~10GtC/yr). Pumping proceeded for 50 years which would yield roughly the required amount of negative emissions called for by most RCP2.6 pathways. We also investigated lower and higher pumping rates up to 10GtCeq/yr to examine the effect on pH and carbonate saturation and establish a way to estimate a reasonable level of alkalinization without excessively affecting marine ecology. Previous work[31] examined alkalinity addition as high as ~22 GtCeq/yr although such a high rate is unlikely to be practical or ecologically safe. After the 50 year pumping period was over the simulation was allowed to continue up to the 5000-year mark to investigate carbonate compensation and the longevity of the stored carbon. To identify the role of carbonate compensation a control run was performed with sediment compensation turned off. A positive control run was also performed to compare to the case where alkalinity is added at the surface but no compensating acid is deposited at depth, effectively simulating the addition of a fast dissolving alkaline material.

Figure 2a shows that alkalinity pumping results in rapid uptake of CO_2, virtually indistinguishable from simple net alkalinity addition to the surface for the first 50 years. In the subsequent period, the depth of acid release strongly determines the return time and the eventual re-emission of any previously captured CO_2. Injection of acidity in too shallow waters causes reemission within 100-200 years, an insufficient amount of time for any significant amount of carbonate compensation to occur. However, for acid depths greater than 3000m the CO_2 absorbed doesn't begin to be re-emitted for at least 300 years, retaining 85-95% of the absorbed CO_2. For an acidity release below 2000m, the relaxation half-life of CO_2 return to the atmosphere is found to be ~2500 years. This time provides sufficient contact time for deep carbonate dissolution to occur as shown in Figure 2b, with the global calcite dissolution rate increasing by as much as 0.25 GtCeq/yr. We note that the system relaxation time is significantly increased due to this dissolution, as the half life for CO_2 return in the reference simulations without carbonate dissolution was much shorter (~1000 years), depending solely on ocean circulation. We note that because the ocean pH stat is a bidirectional homeostat, the proportion of CO_2 which will be permanently removed depends on the future emissions scenarios and the eventual equilibrium point of the ocean. The method proposed here simply allows the thermostat to respond much more quickly than it would have otherwise done.

Figure 3 tracks median and 95%ile changes in surface and ocean floor pH. See Figure S1 for the corresponding change in calcite saturation. The median surface ΔpH rises rapidly for the first 1-2 years (0.03/yr) but slows within 10 years to a steady rate of 2×10^{-4}/yr, reaching a maximum median ΔpH of 0.022 after 50 yrs. The increased rate of CO_2 dissolution is mostly able to buffer the increase in surface alkalinity. The seafloor pH however continues to decrease throughout the pumping period due to the considerably slower calcite dissolution rate. Despite this, the perturbation is at most -0.15 pH units at its most extreme point. Varying the global pumping rate between 0.3 and 10GtCeq/yr we found a roughly linear dependence of pH and Omega perturbation and pumping rate (Figure 4). The sensitivity of benthic ecosystems to pH perturbation is poorly understood and requires further research. However, seasonal changes in open-ocean pH can be up to 0.2 pH units[36] while diurnal changes in coastal areas can reach as much as a full pH unit[37]. Using this as a guide we suggest that alkalinity pumping at global rates of 1-3GtCeq/yr is likely feasible without excessive stress on marine systems, though this is a critical area in need of further research.

3.2 Location dependence

Uniform pumping is neither practical nor efficient. From a practical perspective, the location of pumping will depend strongly on the mode of deployment (see discussion section). From an oceanographic perspective, both the efficiency of alkalinity compensation at the surface and the timescales of return of acidity from deep waters vary substantially depending on the location in

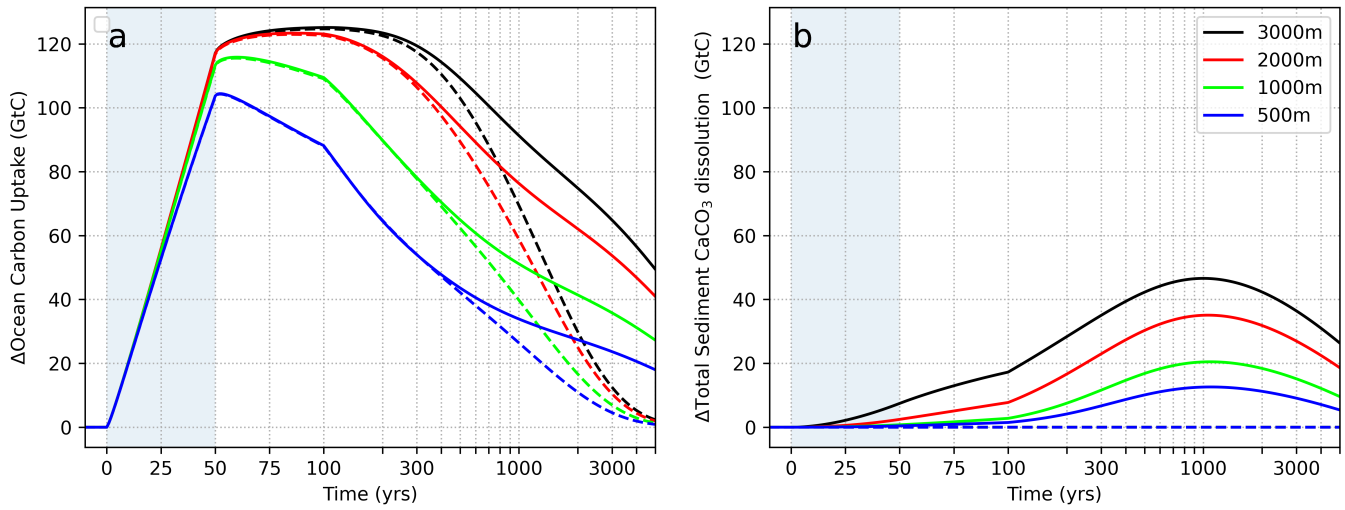

Fig. 2 Shown is the total excess CO_2 uptake and total excess calcite dissolution at the seafloor with respect to time (logarithmic scale past the 100 yr mark). Alkalinity and acidity are separated and pumped uniformly across the ocean, wherever depths permitted, with a total rate of 3GtC equivalent per year. Different colors represent different depths at which acidity was injected. The solid lines represent simulations including carbonate compensation, whereas the dashed lines are simulations ignoring carbonate compensation. Finally a reference simulation is shown where alkalinity is added but no acidity was pumped to depth ("alk only"), representing the effect of adding pure alkalinity to the surface ocean. The grey shading indicates the period for which pumping was active (the first 50yrs). a) Shows the total excess carbon (in GtC) absorbed by the ocean due to alkalinity pumping, relative to a reference simulation without any perturbation. Note that the maximal CO_2 uptake reaches ~85% of the total amount of alkalinity moved (150GtCeq over 50 years), in agreement with the compensation behavior of the carbonate system shown in Figure S0 (see also Renforth et al[13]) . As long as acidity is moved below 2000m, even in the absence of carbonate compensation, the absorbed carbon is retained well beyond 300 years. b) shows the relative increase in global sedimentary carbonate dissolution. When acidity is transported below 3000m about 40% of the absorbed CO_2 is compensated by calcite. Note that the total excess dissolved calcite begins to drop again at ~1000years. This is due to the fact that our simulation kept the atmospheric CO_2 concentration constant at 418ppm, and thus the system begins to return to an equilibrium point where sedimentation rate and dissolution rate balance. The true behaviour of the carbonate homesostate will depend strongly on future atmospheric CO_2 concentrations.

the ocean. The former varies due to differences in the uptake efficiency factor and surface currents, while the latter depends on how soon deep waters are returned to the surface with the global overturning circulation.

The carbonate equilibrium in seawater responds to an increase in alkalinity by shifting towards the carbonate ion. The concomitant reduction in the partial pressure pCO_2 causes an uptake of CO_2 from the atmosphere until equilibrium is restored. The number of moles of CO_2 absorbed for every mole of alkalinity added, the uptake efficiency ηCO_2, can be expressed as the ratio of the partial pressure sensitivities of pCO_2 with respect to total alkalinity (Alk) and total inorganic carbon (DIC)[13,32]. This compensation ratio presents a fundamental inefficiency that needs to be taken into account when calculating potential CO_2 uptake of any ocean alkalinization method in addition to any process inefficiencies. The commonly used approximations $DIC \approx [HCO_3^-] + [CO_3^{2-}]$ and $Alk \approx [HCO_3^-] + 2[CO_3^{2-}]$ at typical ocean pH yield a good approximation for the uptake factor: (derivation in supplementary materials).

$$\eta_{CO_2} = -\frac{\partial pCO_2}{\partial Alk} \Big/ \frac{\partial pCO_2}{\partial DIC} \approx \frac{1}{3 - 2DIC/Alk} = \frac{1}{1 + 2[CO_3^{2-}]/Alk} \quad (3)$$

which evaluates to ~0.8 at average surface ocean concentrations of DIC=2000μM and Alk=2300μM. The intuition why ηCO_2 is smaller than 1 is that while each mole of additionally absorbed CO_2 will be neutralized by one mole of OH- to bicarbonate, some fraction will consume a mole of OH- to become a carbonate ion. A full carbonate model[19,20] was used to calculate the plot in supplementary figure S1, showing that this uptake factor varies substantially depending on the latitude and is one factor to inform optimal alkalinity release locations. Alkalinity addition to areas with high efficiency factor will cause a greater uptake of CO_2 in the near term, however ocean surface currents will tend to move the uptake towards an average efficiency over time, so longer term efficiency can only be predicted with explicit circulation simulation[30,31]. Furthermore, in our case, the return time of the acidity is dependent on the direction and speed of bottom currents and the proximity to upwelling areas.

We thus performed a grid scan of the ocean, where in each simulation an amount of 100Tmol/yr of alkalinity (0.12 GtCeq/yr) was pumped at any one grid point only. Altogether ~1000 independent simulations were conducted, one for every gridpoint with sufficient depth to inject acidity. In each case the entire ocean biogeochemistry was monitored compared to a reference simulation with no pumping.

Figure 5 and supplementary figure S3 show the normalized total uptake of CO_2, such that a value of 1.0 represents an ocean uptake equimolar to the amount of alkalinity pumped. Previous work that examined alkalinity addition in different coarse latitude bands[21] found not all areas are equally efficient at CO_2 uptake or retention. We extend this work with a finegrained map and find

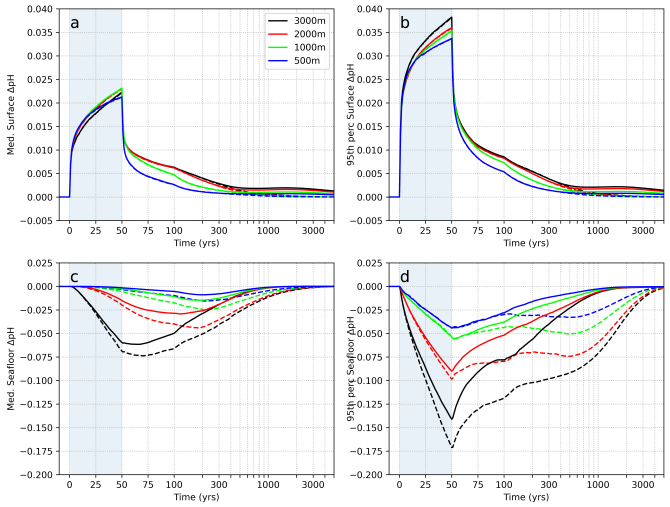

Fig. 3 Median and 95%ile changes in pH at the surface (a&b) (increase in pH) and at the seafloor (c&d) (decrease in pH) for the same runs. It can be seen that even in locations of most extreme pH change, the localized pH changes are not excessive. The changes at the surface are smaller than at depth (despite originating in a much thinner slice of water) because the lowered partial pressure of CO_2 immediately pulls in more carbon due to the relatively fast equilibration time of ∼250 days. At depth the compensation with carbonate deposits proceeds much more slowly and therefore the pH response to acidity pumping is larger over time. Figure S1 shows the equivalent plots of median and 95%ile changes in calcite saturation (Ω).

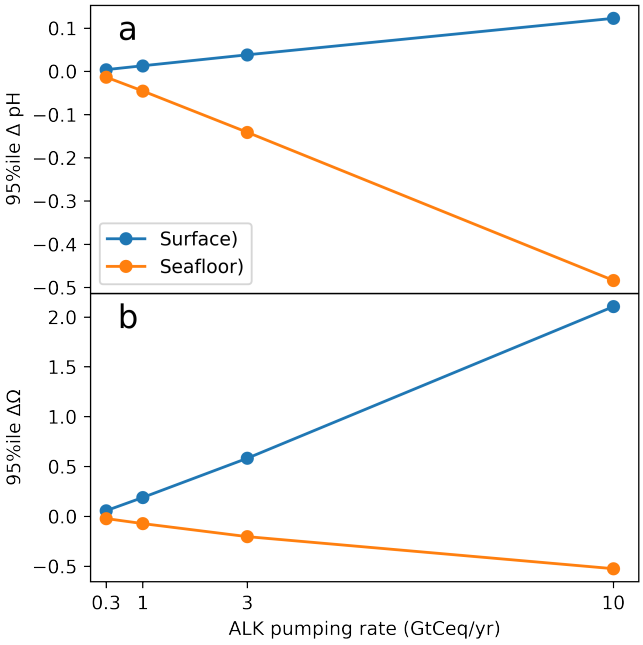

Fig. 4 a) 95i%ile pH changes at the end of 50yr alkalinity pumping across surface and across ocean seafloor for uniform alkalinity pumping at different global rates. b) Likewise, median changes in calcite saturation (Ω), relative to reference simulation. A roughly linear dependence with respect to alkalinity pumping rate is observed.

that on short timescales the efficiency is dominated by the surface efficiency, and the local atmospheric pCO_2. However, after some time surface currents spread the excess surface alkalinity and the effect becomes less pronounced. For the case of alkalinity addition (rather than pumping) most of the locations eventually reach close to the full average efficiency of 0.85 except areas of significant downwelling in the polar regions (see Supplementary Figure S2). The alkalinity is pulled downwards and removed from the surface as is evident in depth plots of calcite saturation (Supplementary Figure S3). In the case of acidity pumping the behaviour is very similar, but on longer timescales, uptake efficiency becomes dominated by the rate of acid return. Since deep return currents generally move southwards, injection of acidity in the northern hemisphere appears to be significantly more efficient in the long run, with some small areas as notable exceptions. Two large areas in the southern ocean appear to return acidity faster than others and are inefficient locations for alkalinity pumping (Figure 5). Figure S2 gives detailed plots of the total excess absorbed CO_2 due to pumping at a selected number of locations.

3.3 Impact on surface and deep water pH

Understanding the pH sensitivity of different locations allows optimization of the alkalinization strategy to minimize ecological effects and costs while maximizing CO_2 uptake.

At the surface, the pH increase will be highest right at the injection site, decreasing exponentially with distance. The alkalinity will be compensated by CO_2 uptake, but depending on the currents and eddy diffusivities which transport and distribute the alkalinity, as well as wind speeds, surface agitation and local atmospheric CO_2 concentration, we can expect different sensitivities at different injection sites. It is important to avoid too large a pH change both for ecological reasons as well as needing to avoid triggering inorganic precipitation[38] of $CaCO_3$. At depth, the injection of acidity must also be considered against an ecological safety margin. We propose that the acidity is injected no closer than 500m to the seafloor and at least 2000m from the surface. This area of the ocean is the least populated by marine species and thus gives ample time for the acidity to dilute horizontally away from the diffuser pipes. Figure 6 shows the sensitivity of surface and deep water pH on the pumping location from ∼2000 individual simulations of single-point alkalinity pumping. The sensitivity ($m^2\,s\,mol^{-1}$) was calculated by dividing the maximal ΔpH observed for any given simulation by the pumping rate density ($mol\,m^{-2}\,s^{-1}$). As expected, areas with stronger surface currents spread surface alkalinity most efficiently, reducing the pH impact at the release location. This effect would be less pronounced if the release stations were free floating with these bulk water movements; however, the horizontal eddy diffusivity is considerably larger in these currents, which would make them preferential release sites nevertheless. Another factor reducing surface pH impact are wind speeds, which reduce the ocean-atmosphere CO_2 equilibration time. The circumpolar wind band likely accounts for the low surface sensitivities observed in the southern ocean (Figure 6, S4).

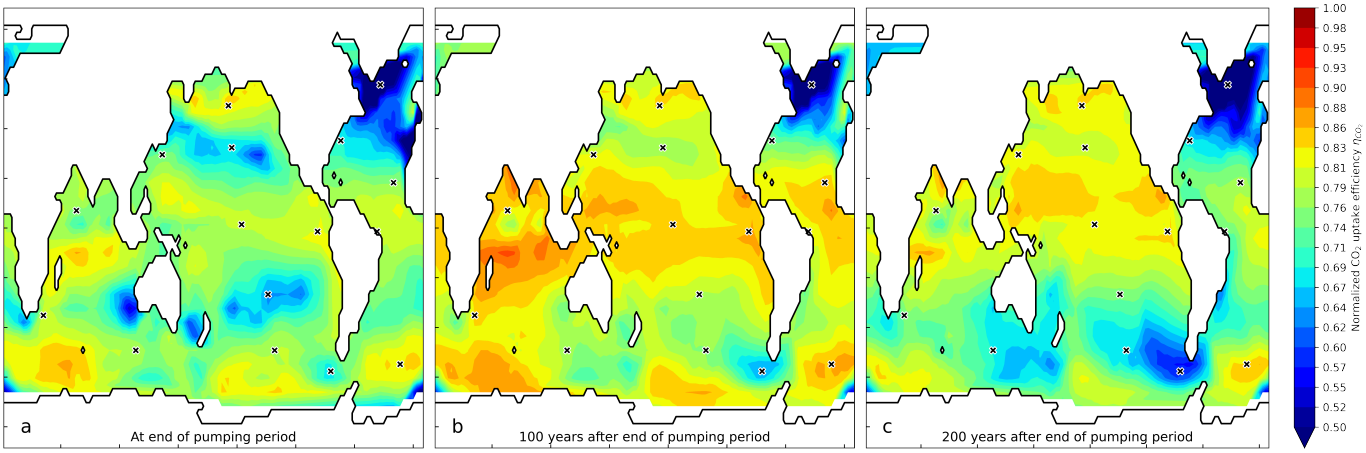

Fig. 5 Efficiency of alkalinity pumping (η_{CO2}) as a function of latitude and longitude. Here (η_{CO_2}) is the number of moles of excess CO_2 absorbed by the ocean normalized by the number of moles of alkalinity pumped. Each point on the grid represents an entire ocean simulation in which 1Tmol/yr were pumped at that point only (a total of ∼2000 simulations). Mapped is the relative increase in total oceanic dissolved inorganic carbon (relative to the reference), normalized by the amount of acidity pumped. Three different timepoints are shown: a) Uptake of CO_2 at the end of the 50year pumping period. Significant differences in the effective (η_{CO_2}) are observed, depending on where the alkalinity was pumped, varying from 0.5 to 0.85. The differences during this period are driven primarily by the efficiency of CO_2 uptake, as the distribution closely matches that of simple alkalinity addition. In particular the northern Atlantic exhibits poor CO_2 uptake. b) CO_2 uptake 100 years after the end of pumping. Alkalinity Pumping in most northern hemisphere areas has caught up to an uptake efficiency of 0.85 with equatorial regions exhibiting the best retention. c) 200 years after the end of pumping. The apparent CO_2 uptake is fully dominated by the acid return kinetics (cf Fig. S5, where alkalinity was added instead of pumped). It is apparent that acidity pumping in the southern hemisphere is less efficient, likely due to the fact that ventilation of deep water occurs in the Southern Ocean and thus acidity returns to the surface more rapidly. Conversely the North Pacific retains pumped acidity the best.

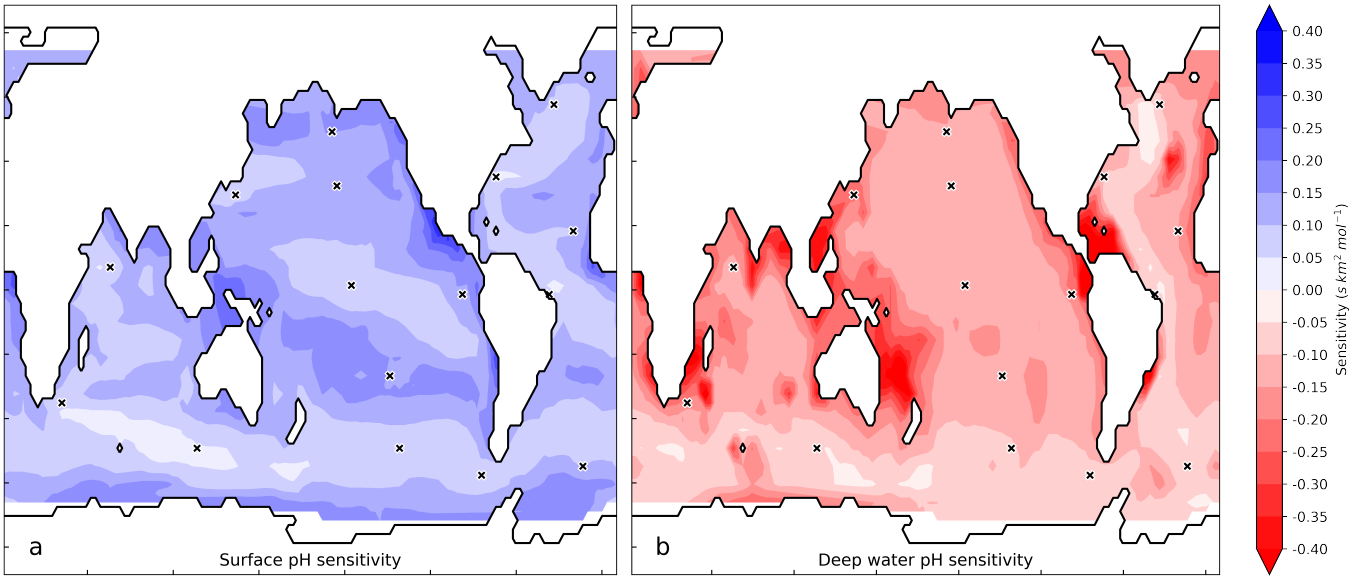

Fig. 6 Local surface pH sensitivity in $\mathrm{s\,km^2\,mol^{-1}}$ obtained by injection at each grid point only (each grid point represents an entire independent simulation). The sensitivity was calculated by dividing the globally maximal ΔpH in either direction observed for any given simulation by the pumping rate density($\mathrm{mol\,km^{-2}\,s^{-1}}$). Panel a) reflects pH changes in the alkaline direction (typically found at the surface release site). The surface sensitivity represents the efficiency with which a stationary addition of alkalinity at any given location with some constant rate is distributed and neutralized by CO_2 invasion. Larger values indicate slower spreading from the release site and/or slower neutralization by CO_2 invasion. Areas with stronger surface currents can spread surface alkalinity most efficiently and are least sensitive to surface pH changes. Panel b) reflects pH changes in the acidic direction (found in deep water where acid is pumped too). The crosses mark the location of the individual plots in Figure S4.

4 Discussion

4.1 Deployment possibilities

The proposed method is only reliant on local resources (seawater) and power and could be implemented in a variety of locations with varying power sources, as shown in Figure 1. Specifically, it would be uniquely matched for untethered power generators, obviating the otherwise arising problem of energy storage or transmission and material transport encountered in other offshore methods[39], providing a productive use of open-ocean power sources in situ. Open-ocean stations could operate on wave, wind or ocean thermal (OTEC,[40–43]) power and could be scaled with a large number of untethered, identical units. Open-ocean photovoltaics have been investigated[44] and trial projects are underway[45]. All of these technologies are still in early development and have not yet benefited from commercial efficiencies of scale and are thus currently relatively expensive. Part of the reason for the lack of wide scale adoption is the need for energy transmission in one form or another. Ocean acidity pumping could thus be a perfect match for these technologies. The lack of need for power transmission or transport can further reduce costs compared to current estimates. Since open ocean is ecologically sparse, alkalinity release in open waters could be less impactful to marine biology than coastal release and could be deployed at larger scale. An alternative approach could involve near-coast operation; larger sized plants could tap into cheap terrestrial energy, especially daytime excess solar. Acid/Base generators could potentially be located just-off-coast with a grid connection to land - transportation of electricity being considerably cheaper than transport of matter, i.e. the pumping of seawater onto land and back should be avoided[46]. Decommissioned oil rigs may offer an ideal platform for such deployment. Coastal locations where the continental slope is close to the coast and strong surface current occur would be ideal, because it shortens the distance acid and base need to be transported, and currents are able to distribute the excess surface alkalinity effectively. A potential intermediate deployment would consist of near-shore wind farms. Where possible, especially in areas where deep waters are not accessible, the acid stream could also be injected underground, into flood basalt formations[47–49] or depleted oil wells where it would react with silicate rocks and be neutralized[16]. Such a deployment could be ideal for example for the North Sea although such areas may be limited to smaller amounts of alkalinity that can be safely released while keeping pH changes below ecological thresholds. However, this could present a feasible method to stabilize ocean pH in localized areas to counteract ecological damage from acidification[50].

4.2 Techno-economic estimation

Although a full techno-economic analysis is beyond the scope of this paper, we conduct a rough estimation of potential costs of electrodialysing seawater using published data from other methods which create pH gradients. Acid/base production could be implemented using either electrolysis or bipolar membrane electrodialysis. Electrolysis was among the first methods suggested for negative emissions technology[16], though the generation of gases is energetically inefficient and has to be either recouped using a fuel cell, adding complexity and cost, or recouped by selling the products[24], which necessitates mass transport of the products[39]. The use of electrolysis on seawater at gigatonne scale may also produce significant quantities of volatile halogenated organics which are ozone depleting, such as bromo- and chloromethane[17]. Here we choose to focus on electrodialysis methods, which have been proposed and tested for seawater CO_2 extraction[51–56]. However, even if colocated with desalination plants, costs are high (373-604\$/tCO_2[52], 540\$/tCO_2 Digdaya 2020) in part due to very large quantities of seawater needing to be processed (about 11,000m^3/tCO_2). In contrast, releasing the alkalinity to the ocean for passive CO_2 absorption and storage is conceptually and technologically simpler, consisting only of the acid/base generator. The quantity of seawater needing to be processed is greatly reduced ($\sim$250m^3/tCO_2 depending on the exact concentration of effluent acid and base). There is no CO_2 extraction, thus saving capital and operational costs of membrane contactors[52]. Indeed Digdaya found membrane contactors and vacuum pumps accounted for 90% of the equipment cost.[55] Instead, leveraging the ocean as a sorbent surface obviates the need for air contactors as well as additional storage, as the CO_2 is stored as relatively benign carbonate ions. From a capital and operational cost perspective, alkalinity pumping is a strict subset of electrodialysis-driven CO_2 extraction and should thus always be cheaper, whether the acidity is moved to deep ocean or underground. The three largest contributors to overall levelized cost would be the cost of electricity to drive the electrodialysis stack, the cost of pre-treating seawater to prevent fouling of the membrane stack and the cost and lifetime of the membranes themselves. Minor contribution costs are the pumping of acidified water to depth. In the open ocean scenario we assume that the cost of the structure are implicit in the assumed levelized costs for open-ocean electricity, and that the electrodialysis apparatus is generally much smaller than the structure. In the following we discuss the likely current ranges of these costs and likely learning curve improvements into the future. However it should be noted that in order to further narrow these estimates, construction of medium-size prototypes[52] is essential.

4.2.1 Energy costs.

In bipolar membrane electrodialysis (BPMED), the thermodynamic minimum energy to create effluent streams at a given pH can be calculated from the Nernst equation as

$$\Delta G = 2.303RT\Delta pH \tag{4}$$

where ΔpH is the pH difference between the acid and base effluents. For a base effluent concentration of 1M NaOH, the minimum energy is $\sim$80kJ/mol ($E^0 \approx 0.83V$) at ambient conditions. A real BPMED stack of course will require considerably more energy due to ohmic losses in the membranes and the thin solution layers, electrolytic losses at the electrodes, and back-leakage of protons or hydroxide ions. Electrodialysis is, in principle, more efficient than electrolysis for creating a pH gradient, since no additional energy is expended to generate

gaseous O_2 or H_2 (E0=1.23V) which has to be recouped economically[39] or via fuelcell[16]. The specific energy consumption (E_{sp}, $kJ\,mol^{-1}$) varies substantially in the literature ranging from 160 to over 350kJ/mol (162kJ/mol[57], 155kJ/mol[55], 242kJ/mol[52], 236kJ/mol[56], 255kJ/mol[58], 259kJ/mol[59], 328kJ/mol[60], 341kJ/mol[61]). This represents process efficiencies of only 20-45%, suggesting that there is potential for learning curves and technological improvements. Many of the above studies aim to valorize reject brines and are optimized to produce both concentrated (>1M) and pure acids and bases for industrial use and thus require deionized water to feed acid and base tanks in feed-and-bleed flow schemes. For purposes of acidity pumping the effluent can be more impure and dilute than in the above studies, affording potentially lower costs. The levelized cost of electricity for free floating power generation is highly variable, and likely suboptimal due to the lack of current economies. Wind power has been estimated at \$30-\$80/MWh[43]. OTEC is estimated to provide energy at a cost of \$150-\$200/MWh[39,42]. Wave power generators levelized costs are highly uncertain and maybe in the range of \$120-\$470/MWh[62]. Even though transmission costs can be saved in our case, the present-day costs are likely too high for economical carbon capture, but have considerable potential for reduction with economies of scale. As an alternative, land-base power could be used in near-coast applications where strong currents allow for nearby alkalinity distribution. Examples include the Agulhas, the Kuroshio, the Gulfstream and the North Brazilian current. However deep-water acid disposal becomes more limited as bottom currents are much slower and it may be better to instead pump the acidified stream underground if suitable basalt formations are available. Utility scale solar is likely the cheapest land-based energy source with unsubsidized levelized costs as cheap as \$32-\$44/MWh and wind at \$28-\$54/MWh[63]. It is thought that there will be a considerable excess of this power during daytime hours, for which finding a carbon negative use would be desirable to help with load leveling.

Assuming an efficiency range of 160-250kJ/mol, energy prices of 30-80\$/MWh and an ocean uptake efficiency ηCO_2 of 0.8 we obtain a range for the energy costs of 38\$-158\$/tCO_2. It is interesting to compare these energy requirements to other CDR approaches. Electrolytic approaches require about ~300kJ/mol[24]. Direct air capture (DAC) has been estimated at 200-1000kJ/mol[64] and more recently at 370-550kJ/mol[65] Energy requirements for methods involving mafic or ultramafic rocks to the ocean, likely needing to be ground to 1μm for open ocean application[21], vary substantially from[15,38] 175-315 kWh/t to[23] 500-1000 kWh/t. Depending on the rock type, with a net uptake efficiency of 0.3-0.8 tCO_2 per tonne of rock, one obtains an energy requirement of 35-528kJ per mol of CO_2 absorbed.

4.2.2 Water pretreatment costs.

As ion-exchange membranes are prone to scaling and fouling[66], methods that electrodialyse seawater typically use nano-filtration (nF) and reverse osmosis (RO) pretreatment to remove divalent ions[51,59], concentrate the input brine and provide deionized water, especially for the base compartment where scaling would be most pronounced. The associated costs are not negligible and tradeoffs need to be considered. Higher flow rates increase pretreatment costs but reduce concentration gradients in the BPMED stack leading to higher faradaic efficiency. There is a tradeoff point, typically around 0.50-1.0M effluent acid/base, corresponding to a pretreated water need of 56-114m^3/tCO_2 (accounting for an uptake factor of 0.8). We estimate the cost of water pretreatment[67] at \$0.5/m^3, leading to a cost range of 28-57\$/tCO_2. Development of BPMED processes which are more resistant to fouling, may mitigate this pretreatment cost.

4.2.3 Bipolar membrane capital costs.

Current densities in BPM stacks vary typically between 450-700 $A\,m^{-1}$ REFS and cell resistivities of 0.003 $\Omega\,m^2$, giving a power density of P_D=1.5-0.6kW/m^2. We can thus calculate the levelized cost contribution of the membranes as $C_M \eta E_{sp}/P_D$, where C_M ($\$s^{-1}\,m^{-2}$) is the levelized discounted cost of the membranes and $\eta = 0.8$ is the CO_2 uptake efficiency. Lower current densities improve the energy efficiency due to lower resistive losses but increase membrane capital costs[60], leading to cost tradeoffs. Reduction of membrane costs by 5x-10x through economies of scale and technological advances thus have the opportunity to drastically reduce energy costs. Commercial bipolar membrane stacks (consisting of one bipolar membrane and two monopolar membranes) are currently produced at relatively small quantities, but at scale, with an assumed active lifetime of about 3 years we could reasonably expect a levelized cost[52,55] of $C_M = 200\$s^{-1}\,m^{-2}$. Thus we estimate the membrane capital cost contribution between \$20-75\$/tCO_2.

4.2.4 Dispersion.

Depending on the deployment mode, the alkalinity and acidity need to be separated and transported. In the case of open ocean deployment, the alkalinity is simply released on site, while the acidity is pumped to depth. We can assume that the capital costs of the floating structure are implicitly included in the levelized cost of the chosen off-shore energy system, as the electrodialysis unit would be quite small compared to the energy structure. We can estimate the additional requirements for pumping as follows. Assuming an acid concentration of 0.5-1.0M, the quantity of water to be pumped is 28-56m^3/tCO_2. As no net work is done against gravity, the energy for pumping is that of overcoming the friction in the pipe. We can estimate the head loss (in meters of water) using the empirical Hazen–Williams equation (in SI units):

$$h_f = 10.67 \left(\frac{Q}{C}\right)^{1.852} d^{-4.8704} L \tag{5}$$

where Q is the flow rate (m^3/s), d and L are the diameter and length of the pipe (m), respectively, and C is an empirical pipe roughness coefficient, about 140 for a typical smooth pipe. For example a 3000m long pipe, 5cm wide, and a flow rate of 5L/s would require a head pressure of ~40bar. This is quite similar to injection of CO_2 into basalt formations requiring ~27m^3/tCO_2 of water and pressures of 25bar[47]. The power needed to pump water at a rate of Q through the pipe is given by:

$$P_{pump} = h_f \gamma_w Q \quad (6)$$

where γ_w is the specific weight of water, 9.8 kN/m^3. The power required to generate the acid and base is given by

$$P_{ED} = c_H E_{sp} Q \quad (7)$$

Where E_{sp} is the specific energy requirement of the BPMED stack (kJ/mol) and c_H is the concentration of acid produced ($c_H = 10^{-pH}$). Assuming for example $c_H \approx$0.75M and $E_{sp} \approx$180kJ/mol we obtain $P_{ED} \approx$ 675kW and $P_{pump} \approx$ 20kW, just 3% of the dialysis energy requirements. However, the engineering requirements for a deep-ocean pipe system are non-negligible, resembling in many ways that of deep ocean lift cables for deep ocean ROV systems in terms of size, design and required resistance to ocean stress. The amortized costs, for a production at scale, are highly dependent on the particular ocean location and mode of deployment and thus difficult to estimate. As an orientation, if we assume conservatively a 5 year lifespan and a cost of 60\$/m for a 2500m pipe we obtain a levelized cost of about \$7.2/tCO_2. However the challenges of open-sea engineering are formidable and pilot studies would be necessary to narrow the cost estimates.

If alkalinity is generated near shore at scale it will need to be dispersed away far from the shore to avoid local pH spikes. However, because the alkalinity is relatively dilute (0.1-1mol/kg) compared to dry solid alkaline materials ($\sim$25mol/kg) bulk transportation is considerably less efficient. For example, at $\eta = 0.8$, 28.4 tonnes of 1mol/kg hydroxide solution are required for every tonne of CO_2 absorbed. Large-scale maritime shipping costs are around \$0.0016-\$0.004/t.km and produce about 7gCO_2/t.km[38]. Assuming alkalinity to be dispersed in a 300km strip around the coast, i.e. within the exclusive economic zone of any bordering country, and typical tanker speeds of 14knots (7.2m/s), a 300km roundtrip (150km zone) could be completed in 12 hours, with a daily turnaround. Assuming a factor of 2 inefficiency compared to ordinary shipping, due to the very frequent loading, we obtain a cost of 13-33\$/tCO_2. Furthermore, as tankers are hard to decarbonize, $\sim$57kgCO_2 are emitted for every tonne of CO_2 absorbed, about a 5% reduction in efficiency. The additional costs and the additional CO_2 impact of transport limit alkalinity release to coastal areas and thus limit the total scaling of landbased alkalinity production.

Overall we obtain a minimum cost per tonne of CO_2 captured of $\sim$\$93-\$297/tCO_2. This estimate is quite close to estimations obtained by a recent study[46,52] (110-325\$/tCO_2) for the BPMED portion of their process, which conducted a much more detailed techno economic analysis for CO_2 extraction. As expected the costs are much lower than estimates for CO_2 extraction (373-604\$/tCO_2[52], 540\$/tCO_2[55])

At the lower end, the total cost estimate has similar-sized cost contributions from energy cost, membrane cost and water treatment cost. Thus to drive down overall costs development and cost reduction is needed in all three areas. Furthermore, as with all ocean CDRs, working with ocean water and in marine environments in general poses significant challenges in terms of corrosion and longevity of the equipment which will need to be addressed for a practical, scalable application.

5 Conclusions

We have explored the feasibility of accelerating the natural compensation of ocean acidification by $CaCO_3$ deposits by artificially pumping excess acidity towards the abyssal $CaCO_3$ sediments. The subsequent alkalinization of the surface would counteract anthropogenic acidification and increase the uptake of significant quantities of atmospheric CO_2. Thus alkalinity pumping could meaningfully contribute to a portfolio of negative emissions technologies. Based on our simulation we estimate 1-3GtC/yr could be removed over a 50yr period, without raising deep water pH excessively. For acid injection depth>3000m we show that carbonate compensation is significantly engaged, permanently removing up to 40% of the absorbed CO_2. Reemission of the remainder occurs ionly after 300 years and slowly over several millenia of gradual outgassing, effectively flattening the curve of the anthropogenic CO_2 shock to the atmosphere. In total up to 150GtC could be removed this way before the end of the century, satisfying requirements for negative emissions laid out by RCP2.6 pathways. What might a scaled up deployment look like? Modern offshore 10MW wind turbines can generate on the order of 50 GWh of energy per year, which could be used to sequester up to 50ktC per year. Thus for a total scale of 1GtC/yr about 20000 of such units would be necessary (i.e. about 200GW of total capacity). Current global offshore wind capacity is expected to reach about 500GW by 2050, thus a goal of 1GtC negative emissions could be feasible.

The pumping of ocean acidity presented in this paper avoids many of the environmental issues with mineral-adding alkalinity methods both in terms of impurity dissolution in the ocean and mining impacts on land. It is conceptually simple and requires only locally available resources (seawater and energy), and is thus uniquely suited to openwater deployment. While in the short term, on-shore electrochemical alkalinization is likely more economical due to the inherent engineering challenges of marine engineering, it is also inherently limited in scale. We have shown that transport of dilute acid or base is not economical beyond 150km away from the production site. Disposal of dilute acid into deep basalt aquifers provides a partial solution but its scaling limits are not well understood. Therefore open-water production of acid and base could supplement terrestrially powered CDR and is an interesting avenue of research despite the usual challenges of marine engineering. Open-water CD also provides a route to make use of otherwise unusable renewable energy, an area of CDR research that has been underexplored. In general, manipulation of acidity/alkalinity as a proxy for CO_2 may be technologically simpler and/or more efficient than manipulation of CO_2 directly, whether the acidity is moved into deep ocean or underground. We also presented the first fine-grained analysis of location dependence of surface alkalinization and show that in the short term there is substantial variation in CO_2 uptake efficiency which will need to be considered in any ocean alkalinization plan, mineral-based or not. As with all ocean-based CDR methods, simulations have inherent limits and the ecological parameters and

limitations require substantial further research and experimentation in meso-scale pilot programs.

Conflicts of interest

There are no conflicts to declare.

Acknowledgements

We thank Matt Eisaman, Ben Saenz, Rob Dunbar, Joel Atwater, Will Regan, Daniel Rosenfeld and Kevin McCloskey for many helpful discussions and comments on the manuscript.

Notes and references

1 S. J. Davis, N. S. Lewis, M. Shaner, S. Aggarwal, D. Arent, I. L. Azevedo, S. M. Benson, T. Bradley, J. Brouwer, Y.-M. Chiang, C. T. M. Clack, A. Cohen, S. Doig, J. Edmonds, P. Fennell, C. B. Field, B. Hannegan, B.-M. Hodge, M. I. Hoffert, E. Ingersoll, P. Jaramillo, K. S. Lackner, K. J. Mach, M. Mastrandrea, J. Ogden, P. F. Peterson, D. L. Sanchez, D. Sperling, J. Stagner, J. E. Trancik, C.-J. Yang and K. Caldeira, *Science*, 2018, **360**, eaas9793.

2 L. T. Bach, S. J. Gill, R. E. M. Rickaby, S. Gore and P. Renforth, *Front. Clim.*, 2019, **1**, year.

3 G. P. Peters, *Nature Clim Change*, 2016, **6**, 646–649.

4 J. E. Dore, R. Lukas, D. W. Sadler, M. J. Church and D. M. Karl, *Proceedings of the National Academy of Sciences*, 2009, **106**, 12235–12240.

5 D. Archer, M. Eby, V. Brovkin, A. Ridgwell, L. Cao, U. Mikolajewicz, K. Caldeira, K. Matsumoto, G. Munhoven, A. Montenegro and K. Tokos, *Annu. Rev. Earth Planet. Sci.*, 2009, **37**, 117–134.

6 D. Archer, H. Kheshgi and E. Maier-Reimer, *Geophys. Res. Lett.*, 1997, **24**, 405–408.

7 D. Archer, H. Kheshgi and E. Maier-Reimer, *Global Biogeochem. Cycles*, 1998, **12**, 259–276.

8 D. Archer, *J. Geophys. Res.*, 2005, **110**, year.

9 N. S. Lord, A. Ridgwell, M. C. Thorne and D. J. Lunt, *Global Biogeochem. Cycles*, 2016, **30**, 2–17.

10 J. L. Sarmiento and N. Gruber, *Ocean biogeochemical dynamics*, Princeton University Press, Princeton, 2006.

11 O. Sulpis, B. P. Boudreau, A. Mucci, C. Jenkins, D. S. Trossman, B. K. Arbic and R. M. Key, *Proc Natl Acad Sci USA*, 2018, **115**, 11700–11705.

12 L.-Q. Jiang, B. R. Carter, R. A. Feely, S. K. Lauvset and A. Olsen, *Sci Rep*, 2019, **9**, year.

13 P. Renforth and G. Henderson, *Reviews of Geophysics*, 2017, **55**, 636–674.

14 F. Montserrat, P. Renforth, J. Hartmann, M. Leermakers, P. Knops and F. J. R. Meysman, *Environ. Sci. Technology*, 2017, **51**, 3960–3972.

15 S. J. Hangx and C. J. Spiers, *International Journal of Greenhouse Gas Control*, 2009, **3**, 757–767.

16 K. Z. House, C. H. House, D. P. Schrag and M. J. Aziz, *Environ. Sci. Technology*, 2007, **41**, 8464–8470.

17 G. H. Rau, S. A. Carroll, W. L. Bourcier, M. J. Singleton, M. M. Smith and R. D. Aines, *Proceedings of the National Academy of Sciences*, 2013, **110**, 10095–10100.

18 P. Ziveri, B. de Bernardi, K.-H. Baumann, H. M. Stoll and P. G. Mortyn, *Deep Sea Research Part II: Topical Studies in Oceanography: Topical Studies in Oceanography*, 2007, **54**, 659–675.

19 M. P. Humphreys, L. Gregor, D. Pierrot, S. M. A. C. van Heuven, E. R. Lewis and D. W. R. Wallace, *PyCO2SYS: marine carbonate system calculations in Python*, 2020, `https://zenodo.org/record/3744275`.

20 E. R. Lewis and D. W. R. Wallace, 1998.

21 P. Köhler, J. F. Abrams, C. Völker, J. Hauck and D. A. Wolf-Gladrow, *Environ. Res. Lett.*, 2013, **8**, 014009.

22 *Project Vesta*, `https://www.projectvesta.org/`.

23 J. jie Li and M. Hitch, *Int J Miner Metall Mater*, 2015, **22**, 1005–1016.

24 G. H. Rau, H. D. Willauer and Z. J. Ren, *Nature Clim Change*, 2018, **8**, 621–625.

25 *IPCC special report on carbon dioxide capture and storage*, ed. B. Metz and Intergovernmental Panel on Climate Change, Cambridge University Press, for the Intergovernmental Panel on Climate Change, Cambridge, 2005.

26 P. W. Boyd, A. J. Watson, C. S. Law, E. R. Abraham, T. Trull, R. Murdoch, D. C. E. Bakker, A. R. Bowie, K. O. Buesseler, H. Chang, M. Charette, P. Croot, K. Downing, R. Frew, M. Gall, M. Hadfield, J. Hall, M. Harvey, G. Jameson, J. LaRoche, M. Liddicoat, R. Ling, M. T. Maldonado, R. M. McKay, S. Nodder, S. Pickmere, R. Pridmore, S. Rintoul, K. Safi, P. Sutton, R. Strzepek, K. Tanneberger, S. Turner, A. Waite and J. Zeldis, *Nature*, 2000, **407**, 695–702.

27 S. A. Rackley, *Carbon Capture and Storage*, Elsevier, 2010, pp. 267–286.

28 *Massachusetts Institute of Technology General Circulation Model*, `https://mitgcm.org/`.

29 S. A. S. J. . S. P. Dutkiewicz, S., *A three-dimensional ocean-seaice-carbon cycle model and its coupling to a two dimensional atmospheric model: Uses in climate change studies. Report 122, MIT Joint Program on the Science and Policy of Global Change* , `http://mit.edu/globalchange/www/MITJPSPGC_Rpt122.pdf`, 2005, [Online; accessed 20-April-2021].

30 A. Lenton, R. J. Matear, D. P. Keller, V. Scott and N. E. Vaughan, *Earth Syst. Dynam.*, 2018, **9**, 339–357.

31 M. F. González and T. Ilyina, *Geophys. Res. Lett.*, 2016, **43**, 6493–6502.

32 J. J. Middelburg, K. Soetaert and M. Hagens, *Rev. Geophys.*, 2020, **58**, year.

33 W. M. Berelson, W. M. Balch, R. Najjar, R. A. Feely, C. Sabine and K. Lee, *Global Biogeochem. Cycles*, 2007, **21**, year.

34 B. P. Boudreau, J. J. Middelburg and F. J. R. Meysman, *Geophys. Res. Lett.*, 2010, **37**, n/a–n/a.

35 B. P. Boudreau, *Geophys. Res. Lett.*, 2013, **40**, 744–748.

36 M. Hagens and J. J. Middelburg, *Geophys. Res. Lett.*, 2016, **43**, year.

37 C. E. Cornwall, C. D. Hepburn, C. M. McGraw, K. I. Currie,

C. A. Pilditch, K. A. Hunter, P. W. Boyd and C. L. Hurd, *Proc. R. Soc. B.*, 2013, **280**, 20132201.

38 P. Renforth, *International Journal of Greenhouse Gas Control*, 2012, **10**, 229–243.

39 G. H. Rau and J. R. Baird, *Renewable and Sustainable Energy Reviews*, 2018, **95**, 265–272.

40 J. R. Chiles, *The Other Renewable Energy*, https://www.inventionandtech.com/content/other-renewable-energy-0, 2009, [Online; accessed 20-April-2021].

41 F. Kreith and D. Bharathan, *Journal of Heat Transfer*, 1988, **110**, 5–22.

42 L. Liu, *New Journal of Physics*, 2014, **16**, 123019.

43 A. Babarit, J.-C. Gilloteaux, G. Clodic, M. Duchet, A. Simoneau and M. F. Platzer, *International Journal of Hydrogen Energy*, 2018, **43**, 7266–7289.

44 S. Z. Golroodbari and W. Sark, *Prog Photovolt Res Appl*, 2020, **28**, 873–886.

45 B. Willis, *The Race Is On for Commercial Deployment of Solar in Open Seas*, https://www.greentechmedia.com/articles/read/race-on-for-commercial-deployment-of-solar-in-open-seas, 2021, [Online; accessed 20-April-2021].

46 M. D. Eisaman, *Joule*, 2020, **4**, 516–520.

47 J. M. Matter, W. Broecker, M. Stute, S. Gislason, E. Oelkers, A. Stefánsson, D. Wolff-Boenisch, E. Gunnlaugsson, G. Axelsson and G. Björnsson, *Energy Procedia*, 2009, **1**, 3641–3646.

48 B. P. McGrail, H. T. Schaef, A. M. Ho, Y.-J. Chien, J. J. Dooley and C. L. Davidson, *J. Geophys. Res.*, 2006, **111**, n/a–n/a.

49 D. S. Goldberg, T. Takahashi and A. L. Slagle, *Proceedings of the National Academy of Sciences*, 2008, **105**, 9920–9925.

50 E. Y. Feng, D. P. Keller, W. Koeve and A. Oschlies, *Environ. Res. Lett.*, 2016, **11**, 074008.

51 M. D. Eisaman, J. L. Rivest, S. D. Karnitz, C.-F. de Lannoy, A. Jose, R. W. DeVaul and K. Hannun, *International Journal of Greenhouse Gas Control*, 2018, **70**, 254–261.

52 C.-F. de Lannoy, M. D. Eisaman, A. Jose, S. D. Karnitz, R. W. DeVaul, K. Hannun and J. L. Rivest, *International Journal of Greenhouse Gas Control*, 2018, **70**, 243–253.

53 H. D. Willauer, F. DiMascio, D. R. Hardy and F. W. Williams, *Energy Fuels*, 2017, **31**, 1723–1730.

54 B. D. Patterson, F. Mo, A. Borgschulte, M. Hillestad, F. Joos, T. Kristiansen, S. Sunde and J. A. van Bokhoven, *Proc Natl Acad Sci USA*, 2019, **116**, 12212–12219.

55 I. A. Digdaya, I. Sullivan, M. Lin, L. Han, W.-H. Cheng, H. A. Atwater and C. Xiang, *Nat Commun*, 2020, **11**, year.

56 F. Sabatino, M. Mehta, A. Grimm, M. Gazzani, F. Gallucci, G. J. Kramer and M. van Sint Annaland, *Industrial & Engineering Chemistry Research*, 2020, **59**, 7007–7020.

57 J. R. Davis, Y. Chen, J. C. Baygents and J. Farrell, *ACS Sustainable Chemistry & Engineering*, 2015, **3**, 2337–2342.

58 J. Farrell and S. Snyder, *Bipolar Membrane Electrodialysis for Zero Liquid Discharge Water Softening and Wastewater Reclamation*, https://west.arizona.edu/sites/default/files/data/3_Research_Jim%20Farrell.pdf, 2018, [Online; accessed 20-April-2021].

59 M. Reig, S. Casas, C. Valderrama, O. Gibert and J. Cortina, *Desalination*, 2016, **398**, 87–97.

60 Y. Wang, A. Wang, X. Zhang and T. Xu, *Industrial & Engineering Chemistry Research*, 2011, **50**, 13911–13921.

61 J. Shen, J. Huang, L. Liu, W. Ye, J. Lin and B. V. der Bruggen, *Journal of Hazardous Materials*, 2013, **260**, 660–667.

62 *Annual Report Ocean Energy Systems*, https://report2015.ocean-energy-systems.org/, 2015, [Online; accessed 20-April-2021].

63

64 K. Z. House, A. C. Baclig, M. Ranjan, E. A. van Nierop, J. Wilcox and H. J. Herzog, *Proceedings of the National Academy of Sciences*, 2011, **108**, 20428–20433.

65

66 M. Hansima, M. Makehelwala, K. Jinadasa, Y. Wei, K. Nanayakkara, A. C. Herath and R. Weerasooriya, *Chemosphere*, 2021, **263**, 127951.

67 A. Alsheghri, S. A. Sharief, S. Rabbani and N. Z. Aitzhan, *Energy Procedia*, 2015, **75**, 319–324.

Supplementary material: CO_2 capture by pumping surface acidity to the deep ocean

1 A simple approximation to CO_2 uptake efficiency

Addition of alkalinity to the ocean lowers pCO_2^{oc}, the partial pressure of CO_2, and thus subsequently more CO_2 is taken up from the atmosphere until $pCO_2^{oc} = pCO_2^{atm}$ again. Dissolved inorganic carbon (DIC) exists in the ocean in an equilibrium between the three carbonate species, which can be written:

$CO_2 + H_2O \rightleftharpoons H_2CO_3 \rightleftharpoons HCO_3^- + H^+ \rightleftharpoons CO_3^{2-} + 2H^+$

Introduction of alkalinity consumes H^+ ions and moves the above equilibrium to the right. Under normal ocean pH the vast majority of DIC is in the bicarbonate (HCO_3^-) form, thus addition of alkalinity allows for an approximately equimolar quantity of CO2 to enter from the atmosphere. However the actual amount is slightly smaller than 1: the intuition here is that for every mol of CO_2 entering the ocean we need $\sim$1mol of alkalinity to convert all the CO_2 to bicarbonate, plus additional alkalinity to further convert some fraction to carbonate ions and pull the equilibrium over such that the concentration of CO_2 (and thus pCO_2^{oc}) returns to it's starting value. The unitless uptake efficiency η_{CO_2} can be calculated from the partial derivatives of pCO2 with respect to alkalinity and DIC and represents the slope of the pCO_2 isolines in an Alk vs DIC plot (see Figure S1).

$$\eta_{CO_2} = -\frac{\partial pCO_2}{\partial Alk} \Big/ \frac{\partial pCO_2}{\partial DIC} \tag{1}$$

The carbonate system with equilibrium constants, K0, K1 and K2 is defined as:

$$[H_2CO_3^*] = K_0 pCO_2 \tag{2}$$

$$K_1[H_2CO_3^*] = [HCO_3^-][H^+] \tag{3}$$

$$K_2[HCO_3^-] = [CO_3^{2-}][H^+] \tag{4}$$

where $[H_2CO_3^*] = [CO_2] + [H_2CO_3]$

A full carbonate system yields a complex expression for pCO_2 as a function of *Alk* and *DIC*, but we can easily estimate η_{CO_2} from a common approximation of *Alk* and *DIC*, which assumes that in the ocean $[H_2CO_3^*]$ is not a major contributor to the total inorganic carbon and that several minor species don't significantly contribute to alkalinity:

$$DIC = [H_2CO_3^*] + [HCO_3^-] + [CO_3^{2-}] \approx [HCO_3^-] + [CO_3^{2-}] \tag{5}$$

$$Alk = [HCO_3^-] + 2[CO_3^{2-}] + ... \approx [HCO_3^-] + 2[CO_3^{2-}] \tag{6}$$

Combining all 5 equations, an expression is obtained for pCO_2, where we've contracted all the constants into one constant *K*.

$$pCO_2 = \frac{K_2[HCO_3^-]^2}{K_0 K_1[CO_3^{2-}]} = K\frac{(2DIC - Alk)^2}{Alk - DIC} \tag{7}$$

Differentiating with respect to *Alk* and *DIC*, respectively, yields:

$$\frac{\partial pCO_2}{\partial Alk} = K\frac{(Alk - DIC)^2 - DIC^2}{(Alk - DIC)^2} \tag{8}$$

$$\frac{\partial p\mathrm{CO}_2}{\partial DIC} = K\frac{Alk^2 - 4(Alk-DIC)^2}{(Alk-DIC)^2} \tag{9}$$

Inserting these into the expression for η_{CO_2} and simplifying yields

$$\eta_{CO_2} = -\frac{\partial p\mathrm{CO}_2}{\partial Alk} \Big/ \frac{\partial p\mathrm{CO}_2}{\partial DIC} \approx -\frac{(Alk-DIC)^2 - DIC^2}{Alk^2 - 4(Alk-DIC)^2} = \frac{1}{3-2DIC/Alk} = \frac{1}{1+2[CO_3^{2-}]/Alk} \tag{10}$$

,

which yields ≈ 0.8 for stereotypical ocean values of DIC=2000µM and Alk=2300µM

Thus for every mol of alkalinity added, only $\sim$0.8 mols of CO_2 are absorbed until the partial pressure equilibrium with the atmosphere is restored. This limitation is inherent for all ocean alkalinity methods. A numerical calculation with a full carbonate system yields $\eta_{CO_2} \approx 0.81$ in close agreement the above approximate calculation.

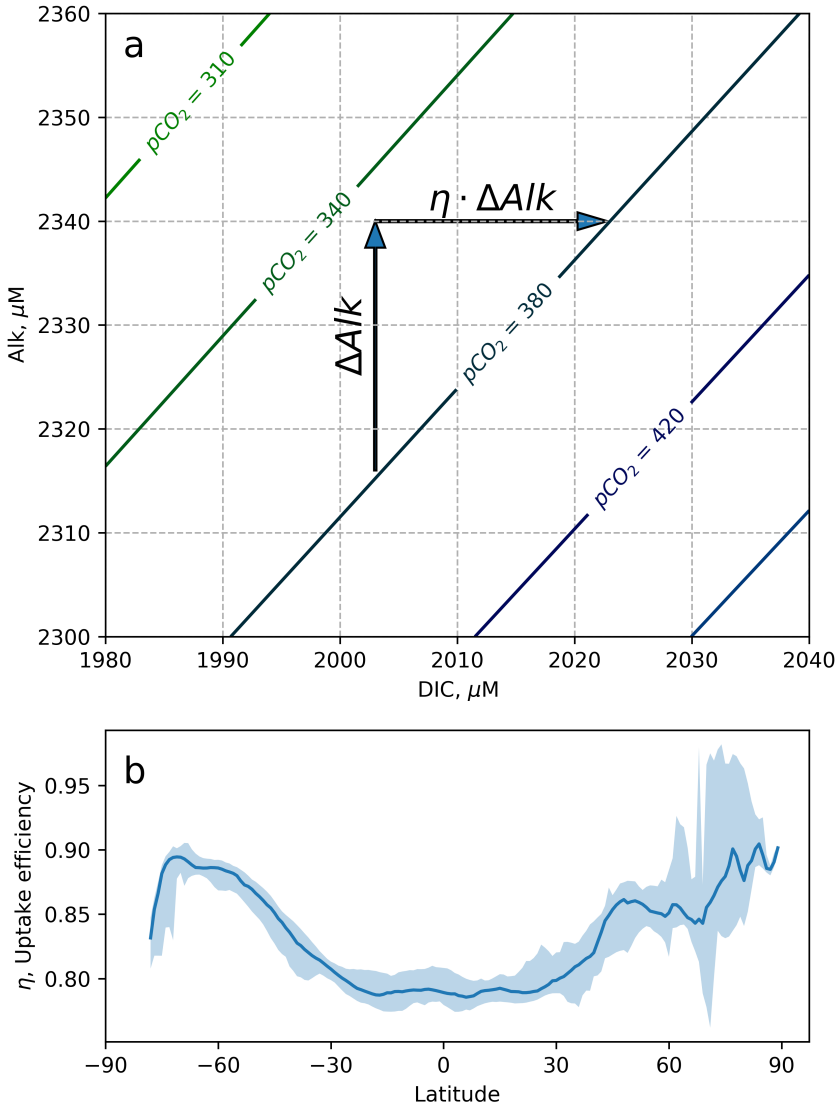

Figure S1 a) Plot of the partial pressure as a function of dissolved inorganic carbon (DIC) and total alkalinity (Alk). Addition of any given quantity of alkalinity ΔAlk to the surface will draw in additional ΔDIC = ηCO_2 ΔAlk until the partial pressure re-equilibrates. b) Graph of CO_2 compensation efficiency ηCO_2 as a function of latitude, calculated from GLODAPv2 data using pyCO2SYS. The worldwide average is ηCO_2= 0.81. Areas of higher efficiency at the poles will take up more CO_2 per mol of alkalinity added to the surface ocean and would a priori be preferred for alkalinization, however the practical amounts also depend strongly on currents, up/downwellings and the atmospheric CO_2 concentrations, thus the true uptake efficiency must be calculated using simulation (e.g. see Figure 5 in main text).

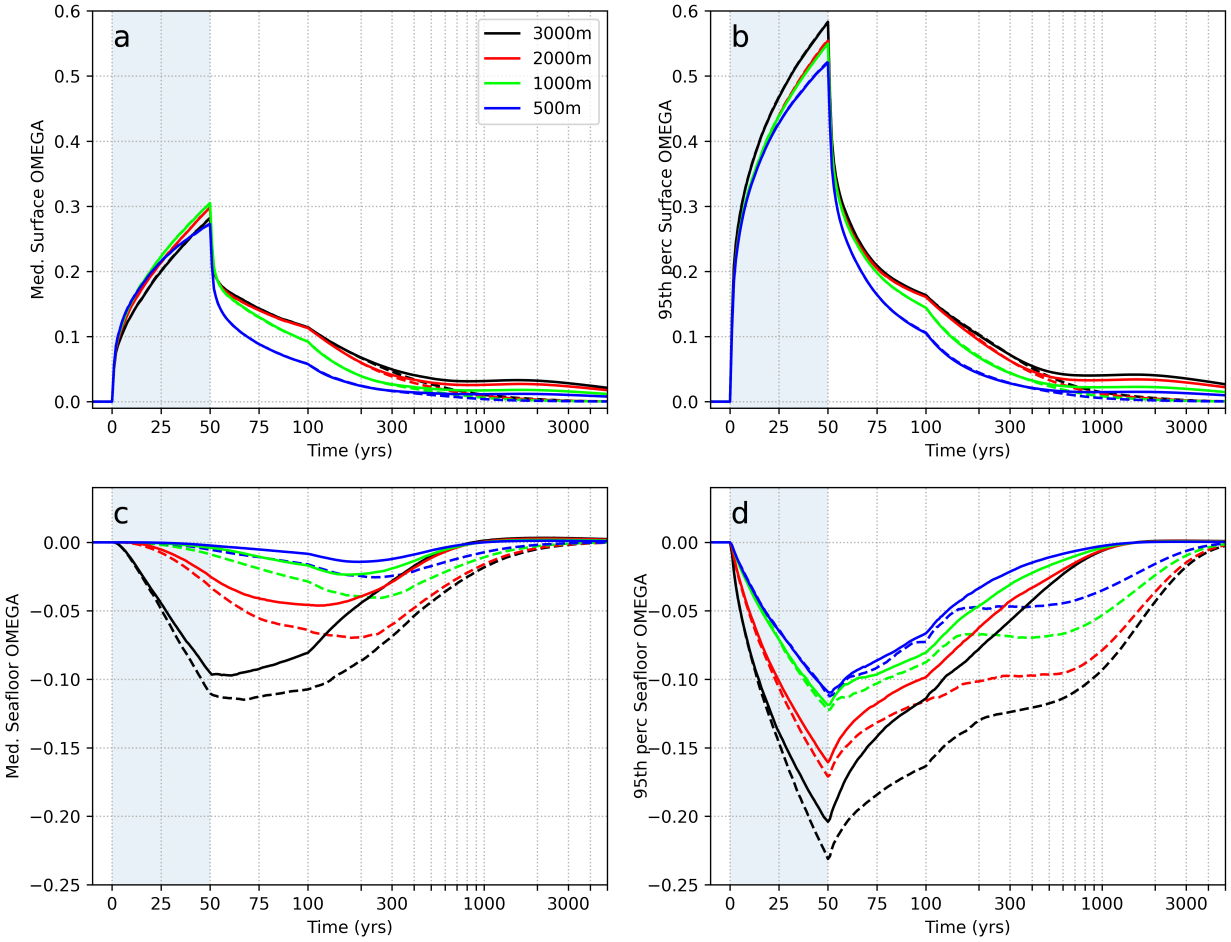

Figure S2 Median and 95%ile changes in calcite saturation (Ω) at the surface (a&b) (increased saturation) and at the seafloor (c&d) (decreased saturation) for the same runs. Analogous to Figure 3 in the main text.

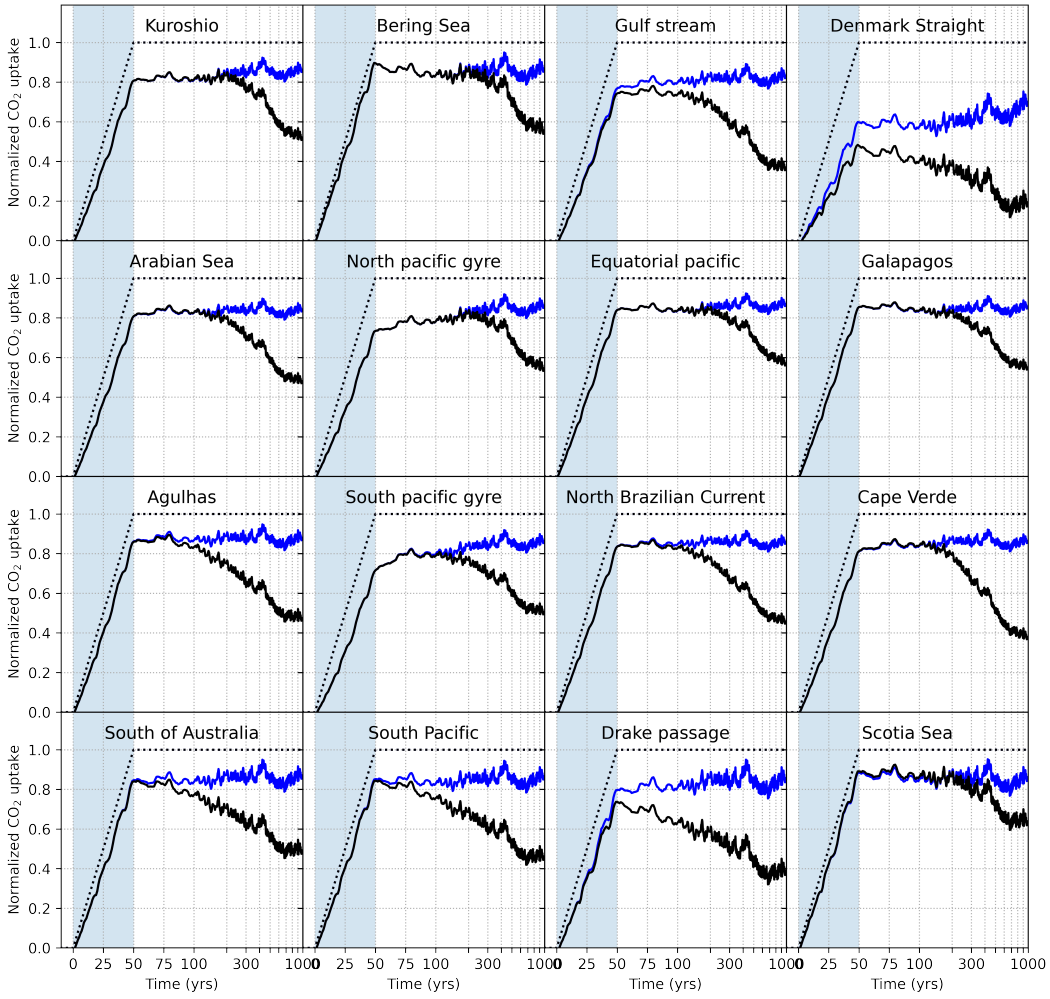

Figure S3 Time-resolved details for individual locations indicated in Figure 5, showing CO_2 uptake relative to the amount of acidity pumped (indicated by the dotted line). The black line shows the behaviour if acidity is pumped to depth and blue if the acidity is removed entirely (simple alkalinity addition). As expected the molar uptake ratio ηCO_2 is 80-85% and then decreases slowly as acidity returns to the surface. However some locations, such as the northern atlantic have markedly lower initial uptake ratios and are unadvisable for acidity pumping or alkalinity addition. Likewise the timescale of acidity return differs significantly depending on location.

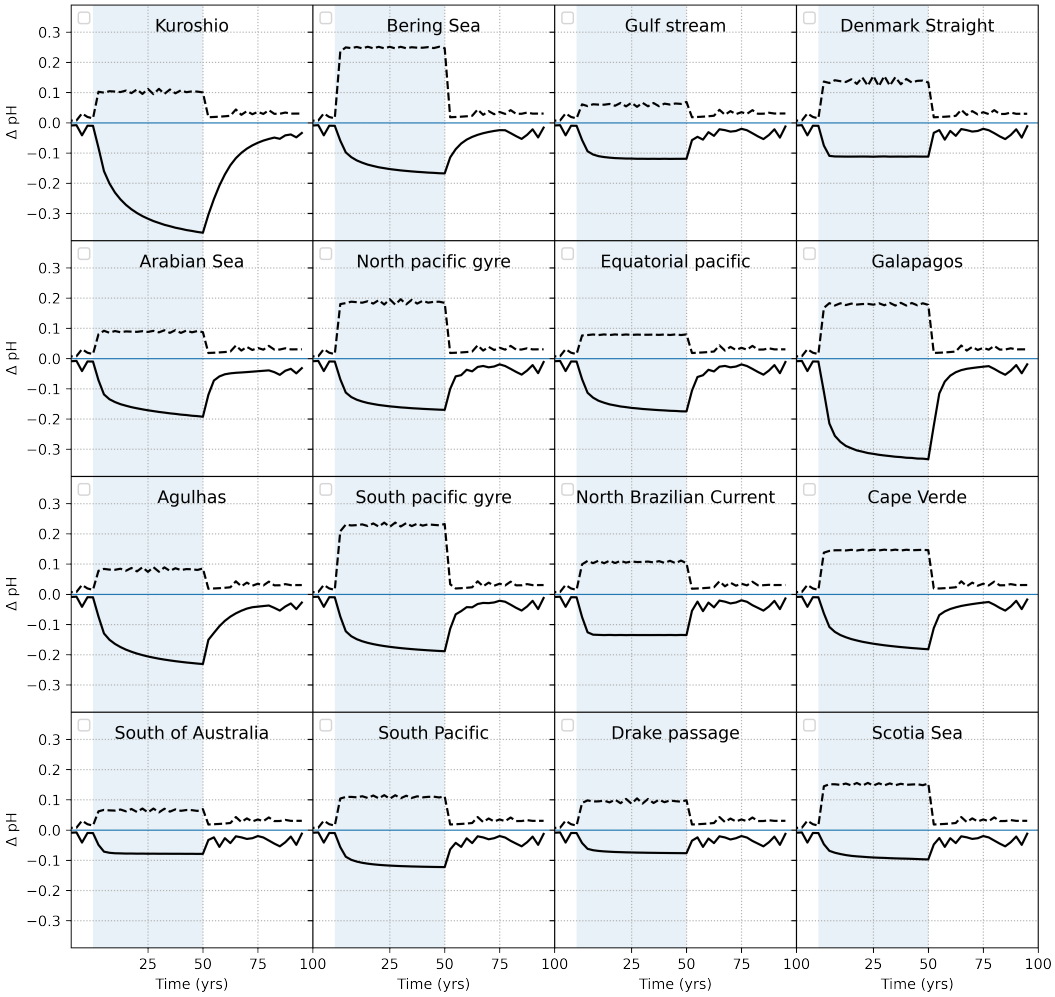

Figure S4 Depth plots of changes in calcite saturation (Ω) at the end of the pumping period (50yrs) for globally uniform acid pumping to 2-3km depth. In some locations, likethe Gulf stream and Denmark Straight, sinking surface waters pull surface alkalinity into deeper waters where it can't be neutralized by atmospheric CO_2 (e.g) and explain the significantly reduced uptake efficiency in these areas (Figure 5, main text). Surface-omega changes are also lower in the southern ocean, perhaps due to the consistent high circum polar winds which reduce the ocean-atmosphere equilibration time for CO_2.

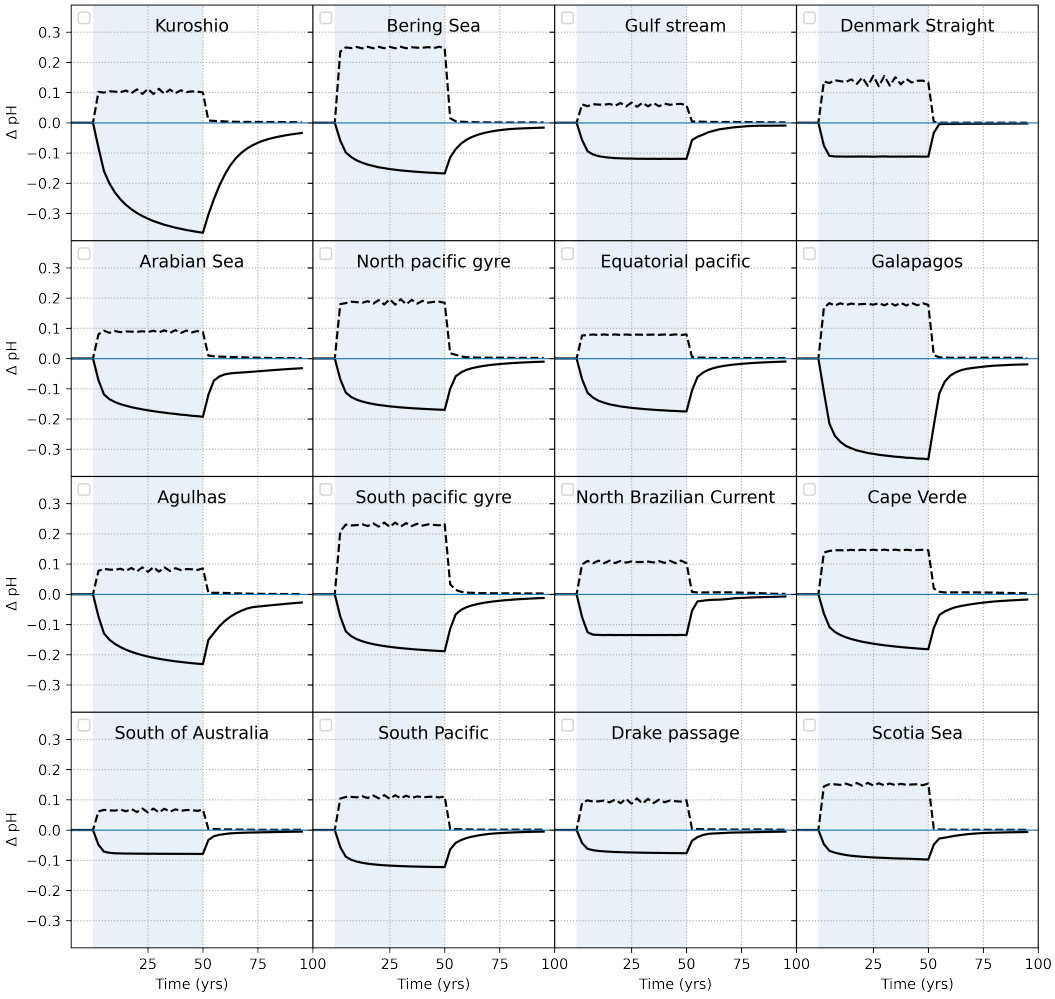

Figure S5 Time-resolved pH changes for individual locations indicated in Figure 5, showing ΔpH extrema at the surface (dashed) and at depth (solid) for the pumping time and 50 years beyond. In each simulation acidity was pumped at just one grid point, with a pumping density of 0.54mol/km2/s (approximately equivalent to 200tC/km2/yr). Note that because in each simulation acidity pumping was only performed at one location, the perturbation can diffuse and dilute horizontally leading to a faster return to baseline than shown in Figure C, where pumping was done uniformly across the entire ocean and at a much larger total rate.

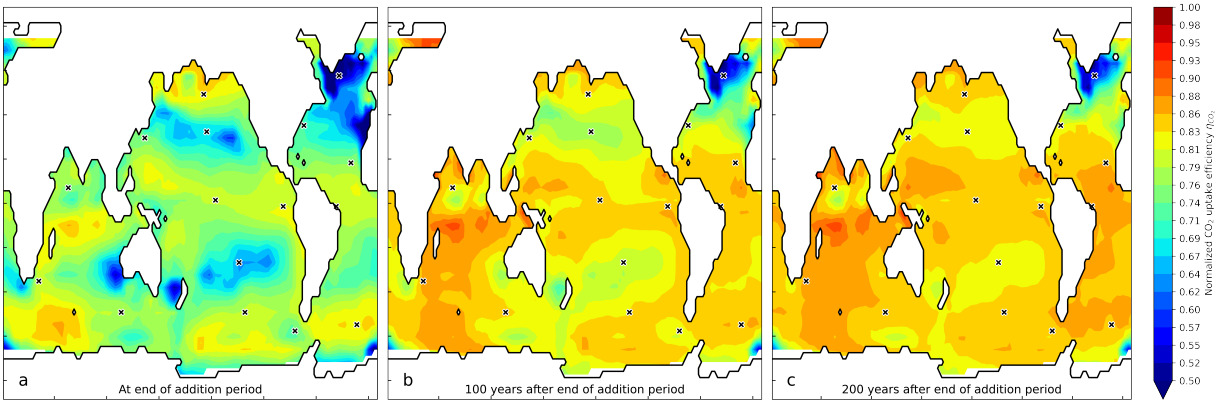

Figure S6 Uptake efficiency upon addition rather than pumping. Analogous to Figure 5 in main text. There exists significant variation in uptake efficiency which any practical ocean alkalinization scheme will need to take into account to maximize early rapid uptake of CO2 and balance against costs of alkalinity transport.